is required in the process of arranging O(1)—O(2) parallel to [001]. In all of these ways all the O atoms in SO_4 must move in order to yield the 'edge-model' structure.

The SO_4 tetrahedra are supposed to be rigid during the phase-transition process and O(2) is more mobile than O(1) as discussed in the present work. The small anharmonic parameters of O(1) suggest that O(1) does not move drastically during the transition. The parameter c_{233} of O(2) is correlated to rotation around a line parallel to [100] through a point lying on the same side as S with respect to O(2). Since the u_2 axis of O(2) is almost parallel to the line between O(2) and the midpoint of O(1)—O(1)′, and O(1) atoms are not expected to move drastically, the positive c_{233} value of O(2) is thought to be correlated to rotation of the SO_4 tetrahedron around the O(1)—O(1)′ edge. The upward and downward rotations with respect to the z direction may occur with equal probability, since there are two negative potential regions at both sides of the O—S bond in Fig. 7, which are equivalent to each other within the present approximation. Thus, the mirror plane at $z = \frac{1}{4}$, which is required by the space group of the high-temperature form, is preserved. This phase-transition mechanism does not contradict evidence obtained in the study of the high-temperature phase and supports the structure of phase I reported in the previous paper (Naruse *et al.*, 1985).

References

ARNOLD, H., KURTZ, W., RICHTER-ZINNIUS, A., BETHKE, J. & HEGER, G. (1981). *Acta Cryst.* B**37**, 1643–1651.
BECKER, P. J. & COPPENS, P. (1974*a*). *Acta Cryst.* A**30**, 129–147.
BECKER, P. J. & COPPENS, P. (1974*b*). *Acta Cryst.* A**30**, 148–153.
BECKER, P. J. & COPPENS, P. (1975). *Acta Cryst.* A**31**, 417–425.
BUSING, W. R. & LEVY, H. A. (1957). *Acta Cryst.* **10**, 180–182.
BUSING, W. R. & LEVY, H. A. (1964). *Acta Cryst.* **17**, 142–146.
CRUICKSHANK, D. W. J. (1961). *J. Chem. Soc.* pp. 5486–5504.
DAWSON, B., HURLEY, A. C. & MASLEN, V. W. (1967). *Proc. R. Soc. London Ser. A*, **298**, 289–306.
EYSEL, W., HÖFFER, H. H., KEESTER, K. L. & HAHN, TH. (1985). *Acta Cryst.* B**41**, 5–11.
ISHIZAWA, N. & KATO, M. (1983). *J. Mineral. Soc. Jpn*, **16**(Special Issue No. 1), 13–20 (in Japanese).
KIRFEL, A. & WILL, G. (1980). *Acta Cryst.* B**36**, 2881–2890.
KIRFEL, A. & WILL, G. (1981). *Acta Cryst.* B**37**, 5298–5302.
MEHROTRA, B. N. (1973). PhD Thesis. Technische Hochschule, Aachen, Germany.
MEHROTRA, B. N. (1981). *Z. Kristallogr.* **155**, 159–163.
NARUSE, H., TANAKA, K., MORIKAWA, H., MARUMO, F. & MEHROTRA, B. N. (1987). *Acta Cryst.* B**43**, 143–146.
SAITO, Y., KOBAYASHI, K. & MARUYAMA, T. (1982). *Thermochim. Acta*, **53**, 289–297.
SAKATA, M., HARADA, J., COOPER, M. J. & ROUSE, K. D. (1980). *Acta Cryst.* A**36**, 7–15.
TANAKA, K., KONISHI, M. & MARUMO, F. (1979). *Acta Cryst.* B**35**, 1303–1308.
TANAKA, K. & MARUMO, F. (1982). *Acta Cryst.* B**38**, 1422–1427.
TANAKA, K. & MARUMO, F. (1983). *Acta Cryst.* A**39**, 631–641.
TOKONAMI, M. (1965). *Acta Cryst.* **19**, 486.
WILLIS, B. T. M. (1969). *Acta Cryst.* A**25**, 277–300.
YAMANAKA, T., TAKEUCHI, Y. & TOKONAMI, M. (1984). *Acta Cryst.* B**40**, 96–102.

Acta Cryst. (1991). B**47**, 588–597

Characterization of Voids in Crystalline Materials: Application to Oxide Ceramic Systems

BY NOEL W. THOMAS

School of Materials, The University of Leeds, Leeds LS2 9JT, England

(*Received* 6 *July* 1990; *accepted* 25 *February* 1991)

Abstract

A computer algorithm has been developed for the characterization of voids in all classes of crystalline materials. From the known atomic coordinates, the centres and radii of all voids can be determined. A given void radius corresponds to the radius of the largest sphere which can be located at its centre, without overlapping of that void sphere with coordinating atoms or ions. The methodology is applied in particular to oxide ceramic systems. Since, in these systems, a useful void is one into which a metal cation may be inserted, it must be coordinated solely by oxygen ions. Three polymorphic oxides are considered in detail: TiO_2, ZrO_2 and WO_3. Dopant ions are identified that are likely to extend the ranges of temperature and pressure over which the individual polymorphs are stabilized. The contribution of the methodology in establishing relationships between chemical composition and crystal structure is also assessed.

Introduction

In most structural studies of crystalline materials, whether metallic, ceramic, polymeric or molecular in nature, attention is focused on the positions and sizes of atoms and ions, with little, or no attention being

0108-7681/91/050588-10$03.00

© 1991 International Union of Crystallography

paid to the unoccupied space between them. This is not surprising, since the determination of atomic and ionic positions, *per se*, is the objective of much experimental crystallographic work. However, when a comparison between different structures is sought, for example in an attempt to rationalize variations in physicochemical properties between one material and another, the characterization of this unoccupied space is potentially of great importance. A novel computational method for doing this is presented here, together with a discussion of its applications to ceramic systems.

The importance of crystalline free space has already been recognized by workers in areas such as shape-selective catalysis and organic solid-state chemistry. For example, many of the catalytic properties of zeolites can be understood in terms of the sizes and connectivity of the pores in the zeolitic framework (Ramdas, Thomas, Betteridge, Cheetham & Davies, 1984). Similarly, the degree of steric control exerted in organic solid-state reactions depends critically upon the degree of intermolecular free space available at reaction centres. It is also conceivable that the transport of molecules to and from reaction centres may take place by means of interconnected pores of molecular dimensions in certain molecular crystals (Gavezzotti & Simonetta, 1987).

Gavezzotti (1983) has taken steps to quantify the unoccupied space in crystals, by means of an computer algorithm. This takes a three-dimensional grid of test points, each point lying either inside an atomic/ionic sphere, or in the space between atoms or ions (henceforth described as 'ions', to reflect the emphasis on ceramic systems). Thus the evaluation of a bulk geometic packing density is permitted, together with a monitoring of local variations in packing density. The algorithm described in this paper is a development of this procedure. Starting from a three-dimensional grid of test points, each point found to lie in the space between ions is used as the starting point of a refinement procedure, in which the maximum spherical void radius in the vicinity of that test point is determined. At the end of the procedure, a list of non-overlapping voids is given, each void being characterized by the coordinates of its centre and a radius.

Although this information is relevant to a wide range of chemical problems, its application to metal oxide (ceramic) systems is emphasized in this article. Just as a consideration of free space permits a rationalization of correlations between chemical composition and crystal structure in certain classes of molecular crystals (Thomas, Ramdas & Thomas, 1985; Thomas & Thomas, 1986), it can also provide insight into relationships between chemical composition and crystal structure in ceramic systems. Attention is also paid to polymorphism, and to the idea of phase stabilization, where the range of temperature and pressure over which a particular type of crystal structure is stable can be extended by doping with ions of varying size and valence.

Computational method

Characterization of the voids in a given crystal structure is carried out by means of an interactive FORTRAN77 computer program written specifically for this purpose, which is run on an Apollo DN3000 workstation at the University of Leeds (Thomas, 1990). The following sequence of operations is performed.

Stage 1

The coordinates of all ions within the unit cell are calculated, together with the coordinates of all ions lying within an adjustable range outside the unit-cell boundaries. This range must be sufficiently large for the coordination environments of all ions within the unit cell to be complete.

Stage 2

A three-dimensional grid of test points is set up, covering one unit cell. The spacing of these test points is governed by a parameter GRSEP, which has been set to 0·2 Å for all the calculations here. The number of equally spaced test points is equal to a/GRSEP parallel to the x axis of the unit cell, b/GRSEP parallel to the y axis and c/GRSEP parallel to the z axis of the cell, where a, b, and c correspond to the lengths (Å) of the three unit-cell axes.

Each test point is monitored to see whether it lies within the spherical volume of an ion, or in the space between ions. The results of this test depend on the set of ionic radii chosen, the choice made here being the radii of Shannon (1976). This parametrization accommodates explicitly the dependence of cationic radii upon coordination number, as well as the smaller variation in oxygen ionic radius between 1·35 and 1·42 Å, as the number of cations coordinating an oxygen ion varies between 2 and 8.

If a test point lies in the space between ionic spheres, then the radius, TPRAD, of that point is given by the distance from the test point to the nearest ionic *surface*. A by-product of this stage is the calculation of the fraction of crystal space occupied by ions, f_{occ}, given by:

$$f_{occ} = N_{intra}/(N_{intra} + N_{inter}). \quad (1)$$

In this equation, N_{intra} is the total number of test points lying *within* ionic spheres and N_{inter} the total number of points lying *between* ionic spheres. Clearly the total number of test points is given by (N_{intra} +

N_{inter}). The accuracy of the value of f_{occ} obtained will increase as the fineness of the grid of test points increases, *i.e.* as the value of GRSEP is diminished.

Stage 3

At the end of stage 2, a list of test points lying between ionic spheres is contained in a temporary file, together with the value of TPRAD for each test point. Those points with TPRAD within a range GRSEP of the maximum value of TPRAD are used as starting points in a refinement, in which the maximum void radii are evaluated. The refinement algorithm proceeds as shown in Fig. 1, where R corresponds to a variable void radius, which is evaluated at different positions. At the initial test point, R = TPRAD. ∇R, or grad R, is the vector giving the direction in which the void radius, R, increases fastest with displacement:

$$\nabla R = \frac{\partial R}{\partial x} + \frac{\partial R}{\partial y} + \frac{\partial R}{\partial z}. \quad (2)$$

The following approximation for ∇R is made in the program:

$$\nabla R = \frac{R(x + \Delta x) - R(x - \Delta x)}{2\Delta x} + \frac{R(y + \Delta y) - R(y - \Delta y)}{2\Delta y} + \frac{R(z + \Delta z) - R(z - \Delta z)}{2\Delta z}. \quad (3)$$

In all calculations here, Δx, Δy and Δz have been set to 0·02 Å in the iterative part of the refinement, and equal to 0·002 Å in the final evaluation of ∇R (Fig. 1).

Stage 4

A test is now carried out for overlapping voids. Each void is regarded as a sphere of radius equal to its optimized radius, R_{final} (Fig. 1), and the test simply monitors overlapping void spheres. In the case of an overlap occurring, the larger of the two voids is retained, with the smaller one disregarded at this stage. The ionic environments of each void are evaluated and printed out for inspection. In the case of an ionic oxide, useful voids (*i.e.* those into which cations may be inserted) correspond to those coordinated only by oxygen ions. If required, polyhedral void volumes may be calculated, corresponding to the volume enclosed by the oxygen ions coordinating the centre of the void (*i.e.* forming a 'coordination polyhedron' around the void). The algorithm required for this has been described previously, in a calculation of the volumes of cation coordination polyhedra (Thomas, 1989, 1991). A void volume defined thus has the advantage of being independent of the values of ionic radii adopted.

Stage 5

The initial scan has identified and characterized all the larger spherical voids in the structure. It may be necessary, however, to identify smaller voids which have been disregarded because they overlap with larger ones. In order to do this, second and subsequent scans are possible, in which voids already identified are regarded as being occupied by spherical *ions* of radius equal to the appropriate void radius, R_{final}. This ensures that these voids will not be detected as such in subsequent scans. Further scans start at stage 1 above, and may be carried out as many times as necessary.

Stage 6

The void positions are identified to ±0·0001 Å by the above procedure. Further precision is possible by the application of equation (3) to the void centres obtained, with successively smaller values of Δx, Δy, Δz, and with smaller translational increments in the iterative procedure shown in Fig. 1.

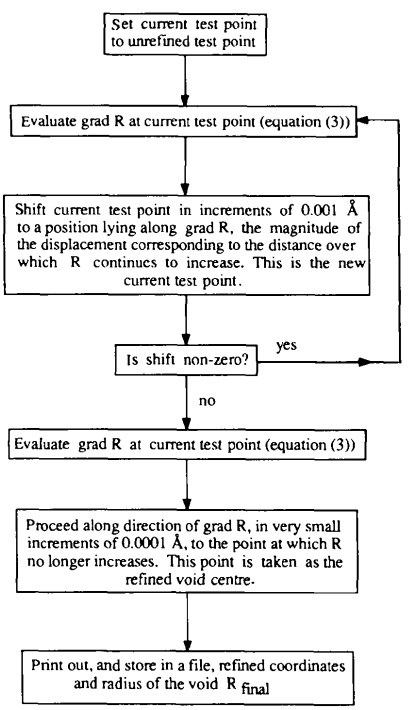

Fig. 1. Schematic diagram of the algorithm to refine the void radius of a test point. Input to the algorithm consists of the coordinates of the test point and its void radius, TPRAD. Output comprises modified coordinates and a refined radius, R_{final}.

Table 1. *Crystallographic data of the structures under examination*

Formula	Phase	Space group	Space-group No.	Z	V_u (Å^3)	N_O	V_{ion} (Å^3)	f_{enc}	E	E^s	T (K)	Ref.
TiO_2	Anatase	$I4_1/amd$	141	4	136·27	6	9·453	0·277	12	4	295	(1)
	Brookite	$Pbca$	61	8	256·84	6	9·758	0·304	12	3	298	(2)
	Rutile	$P4_2/mmm$	136	2	62·42	6	9·904	0·317	12	2	295	(1)
	TiO_2(II)	$Pbcn$	60	4	122·33	6	9·905	0·324	12	2	295	(3)
ZrO_2	Monoclinic	$P2_1/c$	14	4	140·90	7	14·499	0·412	14	7	295	(4)
	Tetragonal	$P4_2/nmc$	137	2	69·83	8	18·969	0·500	14	12	1523	(5)
	Cubic	$Fm3m$	225	4	130·32	8	16·290	0·500	12	12	> 2640	(6)
WO_3	Triclinic	$P\bar{1}$	2	8	421·92	6	9·293*	0·176	12	0	295	(7)
	Monoclinic	$P2_1/n$	14‡	8	423·68	6	9·299†	0·176	12	0	295	(8)
	Orthorhombic	$Pnma$	62	8	430·90	6	8·892†	0·167	12	0	873	(9)
	Tetragonal (1)	$P4/nmm$	129	2	107·91	6	8·992	0·167	12	0	1043	(10)
	Tetragonal (2)	$P4/nmm$	129	2	108·95	6	9·079	0·167	12	0	1223	(10)

References: (1) Burdett *et al.* (1987); (2) Meagher & Lager (1979); (3) Grey *et al.* (1988); (4) Howard *et al.* (1988); (5) Teufer (1962); (6) Wyckoff (1964); (7) Dichl *et al.* (1978); (8) Loopstra & Rietveld (1969); (9) Salje (1977); (10) Kehl *et al.* (1952).

* Mean value: 4 pairs of WO_6 octahedra related by inversion symmetry in unit cell.
† Mean value: 2 sets of symmetry-related WO_6 octahedra in unit cell.
‡ Non-standard setting for space group No. 14.

Table 2. *Coordinates and point symmetries of primary voids in the structures*

Formula	Phase	Space-group No.	f_{occ}	Wyckoff notation and point symmetry		N_O	Coordinates of voids given by computational method x	y	z	Centres of coordinates of oxygen ions coordinating voids x	y	z
TiO_2	Anatase	141	0·64	16(h)*	m	4	0·0	0·6572†	0·0373†	0·0	0·625†	0·0416†
	Brookite	61	0·68	8(c)	1	4	0·5510	0·9473	0·0231	0·5555	0·9400	0·0367
	Rutile	136	0·71	4(d)	$\bar{4}$	4	0·0	0·5	0·25	0·0	0·5	0·25
	TiO_2(II)	60	0·72	4(c)	2	6	0·0	0·6167	0·25	0·0	0·6314	0·25
ZrO_2	Monoclinic	14	0·69	4(e)	1	5	0·8791	0·0259	0·4843	0·9109	0·0486	0·5042
	Tetragonal	137	0·69	2(b)	42m	8	0·0	0·0	0·0	0·0	0·0	0·5
	Cubic	225	0·73	4(b)	$m3m$	8	0·5	0·5	0·5	0·5	0·5	0·5
WO_3	Triclinic	2	0·60	2(i)	1	12	0·0335	0·7220	0·4670	0·0001	0·7501	0·4982
	Monoclinic	14‡	0·60	4(e)	1	12	0·0200	0·2415	0·4701	−0·0010	0·25	0·5028
	Orthorhombic	62	0·59	8(d)	1	12	0·2648	0·0090	0·2502	0·2518	0·0	0·2503
	Tetragonal (I)	129	0·58	2(b)	4$\bar{2}m$	12	0·0	0·0	0·5	0·0	0·0	0·5
	Tetragonal (II)	129	0·57	2(b)	4$\bar{2}m$	12	0·0	0·0	0·5	0·0	0·0	0·5

* Only half of the 16 primary voids in anatase can be occupied simultaneously, owing to the overlapping of pairs of voids.
† This value refers to second setting of space group 141 ($I4_1/amd$), with origin at 2/m.
‡ Data refer to a special setting of space group 14, $P2_1/n$.

Results

Crystallographic data of the three polymorphic compounds, TiO_2, ZrO_2 and WO_3, are given in Table 1. The column headed V_u contains the unit-cell volumes, N_O is the number of oxygen ions coordinating each cation, and V_{ion} represents the volume enclosed by the cation coordination polyhedra in each structure (Thomas, 1989, 1991). The vertices of these polyhedra correspond to the oxygen ions coordinating a given cation, which lies inside the coordination polyhedron. The parameter f_{enc} gives the fraction of space enclosed by the cation coordination polyhedra (Thomas, 1991), which is given here by:

$$f_{enc} = \sum_{i=1}^{z} V_{ion,i}/V_u. \qquad (4)$$

The column headed E gives the number of edges in each coordination polyhedron, and the E^s column gives the number of these edges which are shared with adjacent polyhedra. A variation in E^s is observed between the polymorphs of TiO_2. The column headed T gives the temperature at which the structural data have been collected. These are known precisely for all the structures except cubic ZrO_2, for which no particular temperature has been quoted. In view of the high temperatures required to stabilize the tetragonal and cubic polymorphs of zirconia, recent crystallographic work has utilized dopant ions, in order to stabilize the tetragonal and cubic polymorphs at room temperature (Howard, Hill & Reichert, 1988). The compositions used were $Zr_{0·935}Y_{0·065}O_{1·968}$, which is tetragonal, and $Zr_{0·875}Mg_{0·125}O_{1·875}$, which is cubic at room tempera-

Table 3. *Radii and polyhedral volumes of primary voids in the structures*

Formula	Phase	R_{void} (Å)	$\langle R_{void} \rangle$ (Å)	$\langle R^{cc}_{void} \rangle$ (Å)	V_{void} (Å^3)	V_{void}/V_{ion}
TiO_2	Anatase	0·614	0·614	0·608	2·839	0·300
	Brookite	0·545	0·545	0·542	2·703	0·277
	Rutile	0·460	0·460	0·460	2·726	0·275
	TiO_2(II)	0·600	0·600	0·597	10·484	1·058
ZrO_2	Monoclinic	0·692	0·706	0·693	6·754	0·471
	Tetragonal	0·685	0·884	0·884	18·969	1·000
	Cubic	0·815	0·815	0·815	16·290	1·000
WO_3	Triclinic	0·998	1·342	1·319	43·052	4·633
	Monoclinic	1·068	1·341	1·329	43·923	4·723
	Orthorhombic	1·245	1·329	1·327	44·881	5·000
	Tetragonal (I)	1·285	1·327	1·327	44·961	5·000
	Tetragonal (II)	1·296	1·335	1·335	45·397	5·000

Table 4. *Point symmetries, coordinates and radii of secondary voids*

Formula	Phase	Symmetry-group No.	Wyckoff notation and point symmetry		N_O	Coordinates x	y	z	R_{void} (Å)	$\langle R_{void} \rangle$ (Å)
TiO_2	Anatase	141	16(*f*)	2	4	0·1177*	0·0*	0·0*	0·541	0·541
	Brookite	61	8(*c*)	1	4	0·3398	0·3421	0·3442	0·524	0·524
	Rutile	136	8(*i*)	*m*	4	0·0773	0·6207	0·0	0·428	0·428
	TiO_2(II)	60	8(*d*)	1	4	0·1123	0·6233	0·5889	0·380	0·383
ZrO_2	Monoclinic	14	4(*e*)	1	5	0·3708	0·4880	0·2240	0·568	0·603
	Tetragonal	137	No useful secondary voids							
	Cubic	225	No useful secondary voids							
WO_3	Triclinic	2	2(*i*)	1	12	0·0310	0·2248	0·9661	0·976	1·350
	Monoclinic	14†	4(*e*)	1	12	0·5322	0·2473	0·4886	1·031	1·318
	Orthorhombic	62	No useful secondary voids							
	Tetragonal (I)	129	No useful secondary voids							
	Tetragonal (II)	129	No useful secondary voids							

* This value refers to second setting of space group 141 ($I4_1/amd$), with origin at $2/m$.
† Data refer to a special setting of space group 14, $P2_1/n$.

ture. However, since these relatively large dopant levels are likely to perturb the structures of the pure zirconia polymorphs, they have not been considered in the present study. Data obtained in earlier work on undoped ZrO_2 have been used instead.

Table 2 gives values of f_{occ} [equation (1)] and the coordinates of the primary voids in each of the structures. A primary void is one which has the maximum radius (see Table 3) for that structure, and a secondary void one which has a radius smaller than the maximum (see Table 4). The Wyckoff notation and point symmetries of the voids are inferred from their coordinates, with the assistance of *International Tables for X-ray Crystallography* (1952, Vol. I). Two sets of coordinates are quoted for each primary void. The first of these corresponds to the void centre, as determined from the above computational method, and the second is given by the centre of coordinates of the oxygen ions coordinating each void. They are not necessarily identical to each other. Note that all the primary voids identified in these structures are coordinated by oxygen ions, and not by cations. This is to be expected from the relative numbers of cations and oxygen ions, a factor on which the analysis in terms of cation coordination polyhedra ultimately depends. Further, any potential cationic site (or 'useful void') in an ionic oxide must necessarily be coordinated solely by oxygen ions.

The data in Table 3 refer to the radii and volumes of primary voids. The column headed R_{void} gives the maximum radii of the cations which may be inserted in the appropriate voids without overlapping of cationic and oxygen ionic spheres. These values are generated from the above computational procedure. The value of $\langle R_{void} \rangle$ for a given structure corresponds to the *average* distance from the void centre to the *surfaces* of the oxygen ions coordinating the void. In general, $\langle R_{void} \rangle$ is greater than R_{void}. The quantities in the column headed $\langle R^{cc}_{void} \rangle$ represent the corresponding centre–surface average distances when the centres of coordinates of the oxygen ions (see Table 2) are taken as the void centres. It is observed that $\langle R^{cc}_{void} \rangle$ is

less than $\langle R_{void} \rangle$. Note that the quantity $\langle R_{void} \rangle$ is appropriate for matching cationic radii to void sizes, since the cationic radii of Shannon (1976) are *averages* of the cation–anion surface distances typically found within the coordination shells of cations.

Values of V_{void} correspond to the polyhedral volumes of the primary voids, *i.e.* each void centre is regarded as lying within a coordination polyhedron with vertices given by coordinating oxygen ions. These volumes have been calculated with a separate computer program (Thomas, 1991). The right-hand column of Table 3 gives the ratio of primary void polyhedral volume to cationic polyhedral volume, V_{ion}, for each of the structures. Ratios of polyhedral volumes are discriminating structural parameters, which are useful for a discussion of chemical composition–structure and structure–property relationships in oxide ceramics (Thomas, 1989, 1991).

Fig. 2 illustrates the primary voids in four of the structures, rutile, monoclinic zirconia, cubic zirconia and the lower temperature tetragonal polymorph of WO_3. They are represented as void coordination polyhedra, with the vertices corresponding to oxygen ions.

The data in Table 4 refer to the coordinates and radii of useful secondary voids, *i.e.* those of smaller radius, into which cations may be inserted. Note that there are no useful secondary voids to be found in several structures. Thus once all the primary voids have been filled, there are no remaining voids which are coordinated solely by oxygen ions. Consequently, further insertion, into non-primary voids, is inhibited.

Applications of the methodology to oxide ceramic systems

The above analysis has characterized the voids in three ceramic systems, TiO_2, ZrO_2 and WO_3. It now remains to show how this information is useful in understanding the polymorphism exhibited by these systems, and how it may be exploited to control the

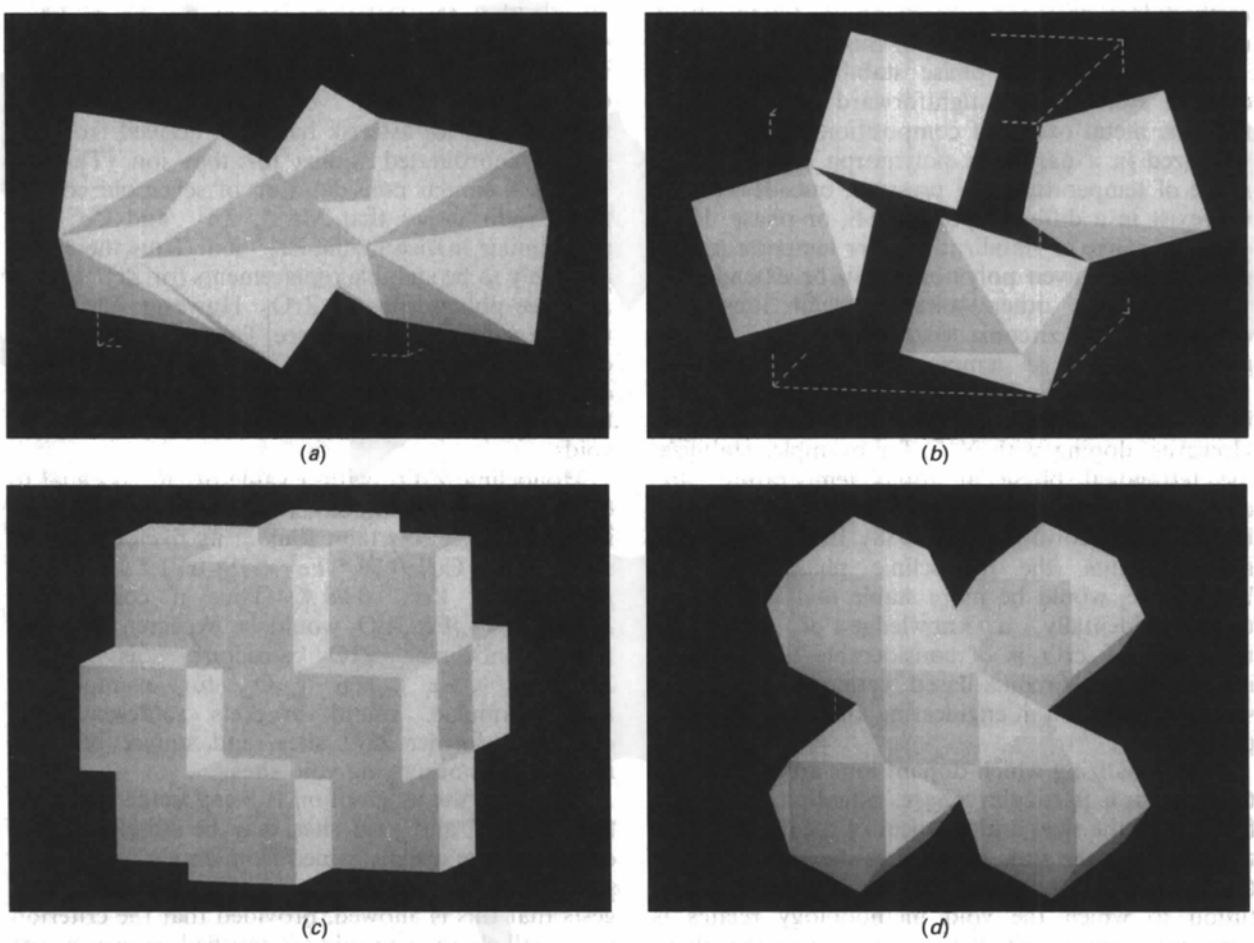

Fig. 2. Coordination polyhedra of the primary voids in four of the systems under study. One unit cell is shown in clinographic projection. (*a*) TiO_2 (rutile); (*b*) ZrO_2 (monoclinic); (*c*) ZrO_2 (cubic); (*d*) WO_3 (tetragonal).

ranges of temperature and pressure over which the different polymorphs are stable. The methodology is also a useful tool for building up an understanding of relationships between chemical composition and crystal structure in metal oxides.

Stabilization of polymorphs over extended temperature and pressure ranges

Much of ceramics science is concerned with identifying the phases present in polycrystalline materials, and with the preparative conditions conducive to obtaining a desirable combination of phases. The use of 'phase diagrams' is widespread in this context, as they permit a rapid assessment of the variation in phase stability with temperature (and pressure), as a function of overall chemical composition, typically within a binary or a ternary system. Although the use of phase diagrams is invaluable for developing an overall picture of a particular system, it does not necessarily lead to an *intuitive* understanding of why a particular composition is to be found in one phase, in preference to another. In contrast, the present methodology provides a starting point for the development of an understanding of this kind.

The basic idea of phase stabilization in oxide ceramic systems is straightforward: a given polymorphic metal oxide, of composition M_xO_y, will be stabilized in a particular polymorph over a limited range of temperature and pressure, outside which it will exist in a different polymorph, or phase. However, the range of stabilization over temperature and pressure of a given polymorph can be extended by 'alloying' with other suitable metal ions. For example, in the zirconia system, tetragonal ZrO_2 is normally stable at temperatures higher than *ca* 1450 K, and cubic ZrO_2 is stabilized only at even higher temperatures, greater than *ca* 2640 K. However, doping with Y^{3+}, for example, stabilizes the tetragonal phase at room temperature, and doping with Mg^{2+} stabilizes the cubic phase at room temperature (Howard *et al.*, 1988). In the absence of these dopants, the monoclinic phase of ZrO_2, baddeleyite, would be more stable at this temperature. Incidentally, a knowledge of the phase behaviour of ZrO_2 is of considerable technological interest, since zirconia-based ceramics find widespread application in engineering and electrical components.

In rationalizing which dopant ions are most likely to stabilize a particular phase, attention should be focused on the sizes and valences of the dopant ions, together with the sizes of the sites they may enter in the host oxide structure. The mode of dopant substitution to which the void methodology relates is necessarily one in which the structure of the phase being stabilized is conserved, *i.e.* the pattern of substitution is such that no oxygen ion vacancies are introduced as a result of the doping. The presence of such vacancies would be associated with local structural perturbations, so that the calculated void sizes would be inapplicable.

Thus yttria-stabilized zirconia, as conventionally prepared, is not structure conserving. The composition studied by Howard *et al.* (1988), $Zr_{0.935}Y_{0.065}O_{1.968}$, contains oxygen vacancies in the parent ZrO_2 structure, as does the composition analysed by Morikawa *et al.* (1988), $Zr_{0.94}Y_{0.06}O_{1.97}$, in an EXAFS study. Similarly, the stabilized cubic phase studied by Howard *et al.*, $Zr_{0.875}Mg_{0.125}O_{1.875}$, contains oxygen vacancies. Clearly, a structure-conserving mode of substitution requires co-doping of two or more ions. For example in the ZrO_2 system, one dopant ion would replace a Zr^{4+} ion, and the other(s) would occupy voids in the ZrO_2 structure. By ensuring that the sum of the valences of the doping ions were equal to four, the valence of the Zr^{4+} ion being replaced, no oxygen ion vacancies would be created.

An examination of ionic radii (Shannon, 1976) reveals that the following common ions of lower valence, in eightfold coordination, have radii closest to that of Zr^{4+} (0·84 Å): Cr^{2+}(LS) 0·83;* Cu^{2+} 0·83;* Ag^{3+} 0·86;* Sc^{3+} 0·87 Å. [Each ionic radius marked wtih an asterisk has been derived from the sixfold coordinated radius for that ion (Thomas, 1991).] A similar consideration of sevenfold coordinated radii shows that Mg^{2+}, Zn^{2+} and Co^{2+} are also similar in size to the Zr^{4+} ion. Thus these ions are likely to be suitable replacements for Zr^{4+} ions in all three polymorphs of ZrO_2. However, the variation in values of $\langle R_{void} \rangle$ (see Table 3) between the different polymorphs of ZrO_2 implies that the various phases are likely to exhibit different preferences towards the co-doping ions which may enter the voids.

Monoclinic ZrO_2, with a value of $\langle R_{void} \rangle$ equal to 0·706 Å, can accommodate most easily the following ions of valence less than four in its fivefold coordinated voids: Cu^{+} 0·70;* Fe^{2+}(HS) 0·71;* Li^{+} 0·69;* Ag^{3+} 0·68;* Zn^{2+} 0·68 Å. Thus a composition $Zr_{1-x}(Cu^{2+})_x[Fe^{2+}]_xO_2$ would be expected to adopt the monoclinic ZrO_2 structure, as would $Zr_{1-x}(Sc^{3+})_x[Cu^{+}]_{x/2}[Zn^{2+}]_{x/4}O_2$, for example. In these formulae, round brackets represent ions occupying former Zr^{4+} sites, and square brackets indicate ions occupying void sites.

Note that the assumption is being made that contiguous Zr^{4+} and void sites may be simultaneously occupied. The insight gained from an earlier detailed study of metal oxide structures (Thomas, 1991) suggests that this is allowed, provided that the criterion of overall charge neutrality is satisfied. However, the method cannot predict an upper limit to the degree

of allowed dopant substitution, represented by x: this must be determined by experiment.

A consideration of the tetragonal and cubic phases of ZrO_2 reveals that the sizes of the void sites are identical to those of the Zr^{4+} sites. Consequently, those ions of lower valence most able to enter the void sites will have radii close to that of the Zr^{4+} ion in eightfold coordination (0·84 Å), as quoted above in connection with monoclinic zirconia. Thus compositions such as $Zr_{1-x}(Cu^{2+})_x[Cu^{2+}]_xO_2$ and $Zr_{1-x}(Sc^{3+})_x[Sc^{3+}]_{x/3}O_2$ are likely to be stabilized in the tetragonal or cubic polymorphs, rather than in the monoclinic phase. In searching for ions most likely to cause ZrO_2 to be stabilized in the cubic, rather than the tetragonal phase, it should be noted that $\langle R_{void}\rangle$ is 0·884 Å in the tetragonal phase but 0·815 Å in the cubic phase. Given that the ionic radius of Zr^{4+} is quoted as 0·84 Å, it would seem that ions slightly smaller than Zr^{4+} [*e.g.* Cr^{2+}(LS), Cu^{2+}] would be more easily stabilized in the cubic phase, and ions slightly larger than Zr^{4+} (*e.g.* Ag^{3+}, Sc^{3+}) would be more easily stabilized in the tetragonal phase.

The significance of some ions being prefentially accommodated in the voids of one phase, rather than in another, is that their presence as dopants will increase the likelihood of that particular phase being stabilized over an extended temperature range. This stabilization will have two components: (i) the internal energy of the stabilized phase will be reduced relative to that of the other phases; (ii) the occupation of void sites in the stabilized phase will inhibit kinetically transitions to other phases. This kinetic inhibition is particularly important in phase transitions involving larger ionic displacements, *e.g.* the martensitic transition between monoclinic and tetragonal ZrO_2.

The four polymorphs of TiO_2 have values of $\langle R_{void}\rangle$ lying between 0·460 and 0·614 Å, thereby giving rise to considerable selectivity of the different polymorphs towards the ions which can be accommodated in their void sites. The Ti^{4+} ion is in sixfold coordination in all four phases, and, with a radius of 0·605 Å, it has the following ions of lower valence, which are closest in radius: Co^{3+}(HS) 0·61; Fe^{2+}(LS) 0·61; Ni^{3+}(HS) 0·60; Cr^{3+} 0·615; Ga^{3+} 0·62 Å.

Ions of valence less than 4 closest in size to the fourfold coordinated voids in anatase ($\langle R_{void}\rangle$ = 0·614 Å) are: Cr^{2+} (HS) 0·61;* In^{3+} 0·61;* Cu^{+} 0·60; Pt^{2+} 0·60; Zn^{2+} 0·60 Å.

Ions of valence less than 4 closest in size to the fourfold coordinated voids in brookite ($\langle R_{void}\rangle$ = 0·545 Å) are: Nb^{3+} 0·55;* Ta^{3+} 0·55;* Ni^{2+} 0·55; Cr^{2+}(LS) 0·55;* Ge^{2+} 0·55 Å.*

Ions of valence less than 4 closest in size to the fourfold coordinated voids in rutile ($\langle R_{void}\rangle$ = 0·460 Å) are: Co^{3+}(HS) 0·46;* Fe^{2+}(LS) 0·46;* Ni^{3+}(HS) 0·45;* Cr^{3+} 0·47;* Ga^{3+} 0·47 Å.

Ions of valence less than 4 closest in size to the sixfold coordinated voids in TiO_2(II) ($\langle R_{void}\rangle$ = 0·600 Å) are: Ni^{3+}(HS) 0·60; Co^{3+}(HS) 0·61; Fe^{2+}(LS) 0·61; Cr^{3+} 0·615; Ga^{3+} 0·62 Å.

Thus, for example, if the Fe^{2+}(LS) ion is substituted for the Ti^{4+} ion in each of four polymorphs, $Ti_{1-x}(Fe^{2+})_x[Zn^{2+}]_xO_2$ is likely to be stabilized in the anatase phase, $Ti_{1-x}(Fe^{2+})_x[Ni^{2+}]_xO_2$ in the brookite phase, and $Ti_{1-x}(Fe^{2+})_x[Ga^{3+}]_{2x/3}O_2$ in either the rutile or the TiO_2(II) phase. The uncertainty over whether the last composition promotes stabilization of the rutile or the TiO_2(II) phase is due to the same ions being closest in size to the voids in both polymorphs. [The variation in the ionic radius quoted for a given ion is due merely to the voids in rutile being fourfold coordinated, whereas those in TiO_2(II) are sixfold coordinated.]

In searching for a differential stabilization effect between these two phases, it is pertinent to remark that values of $\langle R_{void}\rangle$ for *secondary* voids differ significantly between the two phases (see Table 4). Rutile, with $\langle R_{void}\rangle$ equal to 0·428 Å, has the following ions of valence less than 4 closest in size to its secondary voids: Ni^{3+}(LS) 0·42 Å;* Fe^{3+}(LS) 0·42 Å;* As^{3+} 0·44 Å;* Mn^{3+}(LS) 0·44 Å.* By comparison, TiO_2(II), with $\langle R_{void}\rangle$ equal to 0·383 Å, has just the Al^{3+} ion, with a radius of 0·39 Å, sufficiently close in size. Thus a composition $Ti_{1-x}(Fe^{2+})_x[Al^{3+}]_{2x/3}O_2$ would be expected to crystallize in the TiO_2(II), rather than in the rutile structure.

The WO_3 polymorphic system does not lend itself to clear prediction of phase-stabilization effects, since the extent of the variation in void sizes between the different polymorphs is limited. This is not surprising, since the topologies of the ions do not change in the different phases. There are simply changes in symmetry. Values of $\langle R_{void}\rangle$ for the primary voids in WO_3 vary between 1·327 and 1·342 Å, so that the following ions are most suitable for insertion in void sites: Ca^{2+} 1·34; Ce^{3+} 1·34; Dy^{2+} 1·35;* La^{3+} 1·36; Cd^{2+} 1·31 Å. Those ions closest in size to the sixfold-coordinated W^{6+} ion (0·60 Å) are: Ni^{3+}, Rh^{4+}, Sb^{5+}, Tc^{5+} (0·60 Å); Ti^{4+}, Co^{3+}(HS), Fe^{2+}(LS), Mo^{5+} (0·61 Å). Thus insertion of Ca^{2+} or Ce^{3+} ions into the primary voids may favour stabilization of the triclinic and monoclinic polymorphs, which have slightly larger values of $\langle R_{void}\rangle$. Conversely, insertion of Cd^{2+} ions into primary voids may stabilize the orthorhombic and tetragonal polymorphs, which have slightly smaller void sizes. However, the secondary voids in monoclinic WO_3, with $\langle R_{void}\rangle$ equal to 1·318 Å, may accommodate the Cd^{2+} ions preferentially. Note that the secondary voids in triclinic WO_3 should also be considered as

possible cationic sites, in particular since $\langle R_{void} \rangle$, at 1·35 Å, is *larger* than $\langle R_{void} \rangle$ for the primary voids, showing the reverse trend compared to R_{void} values. Consequently, Dy^{2+} and La^{3+} ions may be preferentially stabilized in the triclinic phase.

The above identification of doped compositions most likely to adopt one polymorph or another is purely predictive. Clearly, it is desirable to carry out experimental work, to determine the soundness of the methodology. It would also be instructive to ascertain the degree of doping required to produce phase-stabilization effects: whether, for example, this lies in the parts per million or in the atom percent range. In carrying out these experiments, it would also be necessary to monitor the possible introduction of secondary phases, through doping. This would be contrary to the predictions here, which anticipate that the dopant ions will be in solid solution within the parent phase.

Relationships between chemical composition and crystal structure

An overall strategy for analysing relationships between chemical composition and crystal structure in ceramics has been described previously (Thomas, 1991). The contribution of the void methodology should be seen as an *addendum* to this overall strategy, in that it is incomplete by itself.

The strategy relies on the calculation of polyhedral volumes, and ratios between them, as a means of characterizing the structures of ternary ($X_pY_qO_r$) and quaternary ($X_pY_qZ_rO_s$) oxides. The identification of an unknown composition which is likely to crystallize in a structure identical to that of a known composition is based on two premises: (i) the unknown composition must consist of ions with identical ratios of their coordination polyhedral volumes; (ii) the overall constraint of electroneutrality must be obeyed. Clearly, binary oxides, X_pO_q, are not susceptible to this treatment, since *ratios* of polyhedral volumes between different metal ions cannot be defined.

As discussed previously (Thomas, 1991), the electroneutrality condition for a ternary composition such as XY_2O_4, *i.e.* $v_X + 2v_Y = 8$, is satisfied by $(v_X, v_Y) = (0,4)$. Thus this composition can be regarded as a derivative of a *binary* oxide, Y_2O_4, or, more correctly, YO_2. The void methodology permits this structural relationship to be examined from the other perspective: *i.e.* given the known structure of a binary oxide, it may be possible to predict the existence of a ternary oxide, which is formed from the binary oxide by occupation of some or all of its void sites. Thus one may look for parent–derivative relationships between binary and ternary oxides (or, indeed, between ternary and quaternary oxides).

This possibility can be studied briefly by considering the three binary-oxide systems under examination here, TiO_2, ZrO_2 and WO_3. The ratio V_{void}/V_{ion} in Table 3 is a helpful pointer towards identifying possible derivatives of binary structures. In the case of the WO_3 polymorphs, which are topologically identical, values of the ratio equal to, or nearly equal to 5 point to the relationship between the WO_3 and perovskite structures, ABO_3. In the latter, the ratio of A to B polyhedral volumes, V_A/V_B is equal to, or nearly equal to 5 (Thomas, 1989). Thus a perovskite, for example $NaNbO_3$, is formed from the WO_3 structure by substituting Nb^{5+} for W^{6+}, and substituting an Na^+ ion in each of its 12-fold coordinated voids. Note also that $NaNbO_3$ is stabilized in a sequence of phases similar to that of WO_3 as the temperature is varied. V_{Na}/V_{Nb} is equal to 5 only in the cubic paraelectric phase, which is stabilized at 923 K, falling to 4·737 in the room-temperature orthorhombic phase (Thomas, 1989).

TiO_2 and ZrO_2 can also be regarded as parents of possible ternary metal oxides. Tetragonal and cubic ZrO_2, with a V_{void}/V_{Zr} ratio of 1·0000, are clearly able to give derivatives in which the ion filling the voids is identical in size to that replacing the Zr^{4+} ion. It is also possible to conceive of derived *binary* oxides, in which the ions entering the Zr^{4+} and void sites are identical.

The search for structures derived from binary oxides with known V_{void}/V_{ion} ratios may be systematized by employing a computerized search/match procedure similar to one proposed earlier (Thomas, 1991). In a binary oxide, the polyhedral volume of a void may be expressed as $V_{void} = N_{void}\langle R_{void} \rangle^3$, with the polyhedral volume of the metal ions expressed as $V_{ion} = N_{ion}\langle R_{ion} \rangle^3$. Here $\langle R_{ion} \rangle$ is the mean distance from the centre of the ion to the surfaces of the coordinating ions. Thus the empirical parameters, N_{void} and N_{ion} are readily determined for any binary metal oxide structure. Since the ionic radii of Shannon (1976) are available for most ions, values of V_{void}/V_{ion} may be calculated for virtually all the possible pairs of ions, in which one ion occupies all the primary void sites, and the other replaces the metal ion of the binary oxide. $\langle R_{void} \rangle$ corresponds to the ionic radius of the ion entering the void, and $\langle R_{ion} \rangle$ to the radius of the ion substituting the metal ion of the binary oxide. Electroneutrality must, of course, be maintaind, and a minimum allowed O—O distance of 2·5 Å is applied. Suitable pairs of ions are those which give rise to a V_{void}/V_{ion} ratio closest to that of the parent binary oxide. Table 5 summarizes the results of applying this procedure to TiO_2 and ZrO_2 polymorphs, with a maximum allowed deviation of 2% from the ideal V_{void}/V_{ion} ratio.

A word of caution is appropriate at this juncture, since it is impossible to predict whether a particular

Table 5. *Results of the search/match procedure applied to binary oxides* TiO_2 *and* ZrO_2

Binary oxide		Number of hits for 2% tolerance	Examples of derived ternary oxides
TiO_2	Anatase	15	Na_2CoO_2,* K_2HgO_2, Na_2ZnO_2
	Brookite	53	$CuGdO_2$, $TbLiO_2$, $SmCaO_2$
	Rutile	17	Li_2MgO_2, Rb_2BaO_2, K_2SmO_2
	TiO_2(II)	89	$SrPbO_2$, $NaBiO_2$, $NaCeO_2$
ZrO_2	Monoclinic	56	$NaGdO_2$, $NaCfO_2$, $BaSmO_2$
	Tetragonal	59	$PdLiO_2$, $SbLiO_2$, $NaBiO_2$
	Cubic	59	$PdLiO_2$, $SbLiO_2$, $NaBiO_2$

* Co^{2+} ion is in high-spin state.

composition *will* actually adopt the structure derived from the binary oxide. One example in Table 5, $NaBiO_2$, can be derived either from the TiO_2(II) structure, or from the tetragonal/cubic ZrO_2 structure, and the two structures are quite different. Thus the technique is best regarded as as computational tool, to be used in conjunction with experimental structural work. It is also a helpful approach in developing logical connections between observed crystal structures.

References

BURDETT, J. K., HUGHBANKS, T., MILLER, G. J., RICHARDSON, J. W. & SMITH, J. V. (1987). *J. Am. Chem. Soc.* **109**, 3639–3646.

DIEHL, R., BRANDT, G. & SALJE, E. (1978). *Acta Cryst.* B**34**, 1105–1111.

GAVEZZOTTI, A. (1983). *J. Am. Chem. Soc.* **105**, 5220–5225.

GAVEZZOTTI, A. & SIMONETTA, M. (1987). *Organic Solid State Chemistry*, edited by G. R. DESIRAJU, pp. 391–432. Amsterdam: Elsevier.

GREY, I. E., LI, C., MADSEN, I. C. & BRAUNSHAUSEN, G. (1988). *Mater. Res. Bull.* **23**, 743–753.

HOWARD, C. J., HILL, R. J. & REICHERT, B. E. (1988). *Acta Cryst.* B**44**, 116–120.

KEHL, W. L., HAY, R. G. & WAHL, D. (1952). *J. Appl. Phys.* **23**, 212–215.

LOOPSTRA, B. O. & RIETVELD, H. M. (1969). *Acta Cryst.* B**25**, 1420–1421.

MEAGHER, E. P. & LAGER, G. A. (1979). *Can. Mineral.* **17**, 77–85.

MORIKAWA, H., SHIMIZUGAWA, Y., MARUMO, F., HARASAWA, T., IKAWA, H., TOHJI, K. & UDAGAWA, Y. (1988). *J. Ceram. Soc. Jpn Int. Ed.* **96**, 251–256.

RAMDAS, S., THOMAS, J. M., BETTERIDGE, P. W., CHEETHAM, A. K. & DAVIES, E. K. (1984). *Angew. Chem. Int. Ed. Engl.* **23**, 671–679.

SALJE, E. (1977). *Acta Cryst.* B**33**, 574–577.

SHANNON, R. D. (1976). *Acta Cryst.* A**32**, 751–767.

TEUFER, G. (1962). *Acta Cryst.* **15**, 1187.

THOMAS, N. W. (1989). *Acta Cryst.* B**45**, 337–344.

THOMAS, N. W. (1990). Unpublished work.

THOMAS, N. W. (1991). *Acta Cryst.* B**47**, 180–191.

THOMAS, N. W., RAMDAS, S. & THOMAS, J. M. (1985). *Proc. R. Soc. London Ser. A*, **400**, 219–227.

THOMAS, N. W. & THOMAS, J. M. (1986). *Mol. Cryst. Liq. Cryst.* **134**, 155–168.

WYCKOFF, R. (1964). *Crystal Structures*, Vol. 1, p. 243. London: Wiley.

Acta Cryst. (1991). B**47**, 597–608

A New Parametrization for Investigating Relationships Between Chemical Composition and Crystal Structure in Layered ABO_3 Ceramics

BY NOEL W. THOMAS

School of Materials, The University of Leeds, Leeds LS2 9JT, England

(*Received* 1 *October* 1990; *accepted* 25 *February* 1991)

Abstract

The relationship between the layer and framework pictures of layered ABO_3 ceramics is examined, and expressed quantitatively. This permits a calculation of the volumes of cationic coordination polyhedra in terms of AO_3 layer separations and distances between oxygen ions within the layers. Thus the observed stacking sequences (combinations of cubic- and hexagonal-type stacking) can be quantitatively related to the sizes of the cations, and hence chemical composition. Several ABO_3 systems are examined, with Ba^{2+} and Sr^{2+} as A ions. In the (Ba,Sr)RuO_3 system, the occurrence of 9L, 4L and perovskite phases is rationalized in terms of $\langle V_A\rangle/\langle V_B\rangle$ polyhedral volume ratios, and the solubility of different B ions in the 9L $BaRuO_3$ structure is discussed. Considerations of ionic size are generally adequate to understand the structures obtained, except in compounds with the hexagonal barium titanate structure, where metal–metal bonding occurs. The influence of temperature and pressure on stacking sequence is considered, by examining $BaMnO_{3-x}$ and $Ba_{1-y}Sr_yMnO_{3-x}$ compositions. A rationalization in terms of $\langle V_A\rangle/\langle V_B\rangle$ ratios is again found to be appropriate. Whereas the layer picture breaks down

0108-7681/91/050597-12$03.00

© 1991 International Union of Crystallography